Adaptive PI control of wave energy converters with force and motion constraints

Hoai-Nam Nguyen

Adaptive PI Control of Wave Energy Converters with Force and Motion Constraints

Hoai-Nam Nguyen†

***Abstract*—This paper presents the application of adaptive PI control design to a point absorber - wave energy converter (WEC) under force and motion constraints. Adaptive PI control has several features that make it attractive for WEC system. In particular, it has a clear physical interpretation. The "P" component converts the wave energy into useful energy, while the "I" component changes the WEC system natural frequency allowing the absorber to be more in phase with the incoming waves. However, standard adaptive PI control schemes in the literature do not have the ability to incorporate the constraints in the design phase. The main objective of this paper is to fill this gap by proposing a new adaptive PI control law that can take the constraints into account. Simulation results show that the new control law can improve the performance while respecting system limitations.**

***Index Terms*—Wave Energy Converter, Adaptive Control, Force Constraints, Motion Constraints, Wave Force Estimation, Kalman Filter**

I. Introduction

Wave energy converters are devices that convert sea wave energy into useful mechanical and/or electrical energy. Operating the WEC in an optimal fashion is a primary task for WECs to be competitive with other forms of renewable energy such as wind or solar. There are generally two main requirements for designing a control law: i) it should exploit the full absorption potential of an installed WEC; ii) it should respect the device constraints on force and motions.

Several control strategies have been proposed to improve energy extraction, such as latching control [1], simple and effective control (S&E control) [5], multi resonant feedback control [21], model predictive control (MPC) [11], [15], [19], [22]. In latching control, the body is locked at some moments to keep its oscillation in phase with the excitation force. While latching control is promising, its practical implementation may be very challenging. This is due to the requirement for a short-term wave excitation force prediction, and the excessive loads on the latching mechanism [2]. In MPC, the problem of maximizing energy capture and of respecting system mechanical limits can be naturally formulated as a constrained optimization problem. MPC allows to achieve high energy capture. However, the online computational burden for solving the optimization problem at each time instant can be heavy. In [22], a way to reduce the online computational complexity of MPC is proposed. The basic idea is to move as much as possible part of the control computation offline. Note that MPC requires a short-term wave excitation force prediction. If the prediction is not perfect, the MPC performance can be deteriorated quickly. In multi resonant feedback control [21], the strategy consists of three stages. In stage 1, the spectral decomposition of the measurement WEC outputs is performed. In stage 2, a proportional derivative (PD) control law is used for each individual frequency. The PD gains are computed using the standard unconstrained complex conjugate control theory [3], [4]. Then in stage 3, the control feedback is provided by summing all the PD control actions together. The most notable feature of the multi resonant control law is that it does not require the information of the wave excitation force. However, it is not trivial to extend the approach in the presence of constraints. In S&E control, the idea is to generate a high-level reference velocity, and then to use a low-level servo control loop. An "upgraded" version of of the S&E control is presented in [6]. The technique is based on real-time envelop estimation of the excitation force. However, the approaches in [5], [6] can only deal with the position constraints. In addition, note that the developments rely on the standard unconstrained WEC control results in [3], [4]. Consequently, they are not optimal in the presence of constraints.

Another WEC research line is the adaptive control strategy [7], [20]. The approach consists of two stages: offline and online. In the offline stage, the control parameters are optimized for each operating condition, in our case for each sea state. Then in the online stage, the control parameters are adapted as a function of sea state. However, the approach [7], [20] is only able to update the control parameters on a time window that corresponds to sea state average, e.g., about 15-30 minutes interval. Hence, this "intermittent" control strategy is sub-optimal in terms of energy capture. In [13], [16], an improved adaptive control law is proposed. The idea is to update the control parameters in real-time as the sea conditions change continuously. The control strategy has a root in complex conjugate control theory [3], [4]. However, it does not require a short-term wave excitation force prediction as, e.g., in [9], [10]. The PI structure is chosen as it is simple, and it requires only straightforward computations. The adaptive PI control law was tested experimentally in a wave basin at Aalborg University, Denmark [16]. It is shown that it can harvest 57.14% more energy than the intermittent adaptive control law in [20]. However, the technique in [13], [16] does not take the constraints into consideration in the design phase.

We continue the research line [13], [16] in this paper. The aim is to fill the gap of the results in [13], [16]. By considering the force and motions constraints in the design phase, four main features are noted

- We show that the problem of maximizing the harvested average power in the presence of constraints can be recast as a convex optimization problem.
- We show how to obtain a closed-form solution for the optimization problem.

† SAMOVAR, Télécom SudParis, Institut Polytechnique de Paris, 91120 Palaiseau, France hoai-nam.nguyen@telecom-sudparis.eu

- We show that the standard complex conjugate control result in [3], [4] is a special case of our solution where no constraint is considered.
- We give a necessary and sufficient condition for the following question: **"for a given wave, does there exist a linear control law with given force constraints that can keep the WEC position and speed within their limits?"** To the best of the author's knowledge, this is the first time such a result is obtained.

This paper presents a rigorous treatment of some preliminary results in [14]. In [14], the main question is to examine the well known resonance condition in the presence of constraints. This is done by using a semi-definite program to analyze the wave force-to-velocity map. In this paper, the main question is to propose a control law under the force and motions constraints.

The paper is organized as follows. Section II describes the problem formulation and early works on adaptive PI control. Section III contains the main results of the paper. Section III.A explains how to compute the optimal control law for regular waves. Section III.B studies the feasibility problem. Section III.C extends the results in Section III.A and in Section III.B to realistic irregular waves. Section III.D is concerned with the stability analysis of the closed-loop system. In Section IV, simulation results with comparison to earlier solutions are presented. Finally, some conclusions are drawn in Section V.

II. Problem Formulation

A. Point Absorber

In this paper we focus exclusively on a point absorber, which is a subclass of WECs, see Fig. 1. It consists of a float, also called buoy, moving on the ocean surface only in the heave direction. It is axis-symmetric so that the energy conversion rate is the same for waves coming from all directions. The relative motion of the float with the sea bottom can be converted into usable energy through a power take-off (PTO) system.

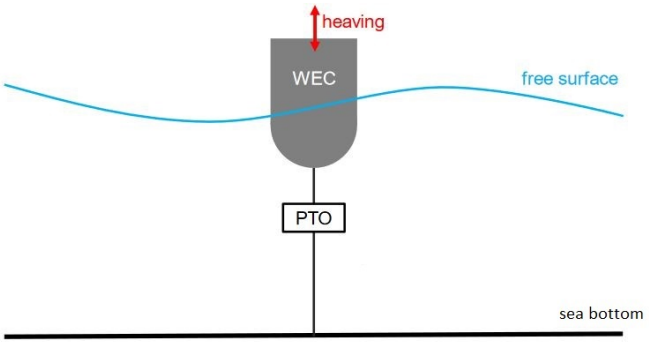

Fig. 1: Schematic diagram of the point absorber.

B. WEC Modeling

It is assumed that the oscillation of the WEC relative to the sea bottom is within some reasonable limit so that the linear theory is applicable [4]. The external forces acting on the WEC are the wave excitation force, and the control force produced by the PTO. Neglecting viscosity, and other losses, the motion of the WEC system can be described in the frequency domain as

$$\left[jwM + \frac{K_{hd}}{jw} + Z_r(jw)\right] V(jw) = F_{ex}(jw) - F_u(jw) \quad (1)$$

where M is the WEC mass, $V(jw)$ is the heaving velocity, $F_{ex}(jw)$ is the wave excitation force on the float, and $F_u(jw)$ is the PTO force. The hydrostatic force gives stiffness force as deviation from hydrostatic equilibrium. It is modeled by the coefficient K_{hd}. The radiation force due to radiated waves is expressed through the radiation impedance $Z_r(jw)$, which is generally decomposed as

$$Z_r(jw) = B(w) + jw\left[M_\infty + M_a(w)\right] \quad (2)$$

where $B(w)$ is the radiation resistance, M_∞ is the added mass at infinitely high frequency, and $M_a(w)$ is the added mass after M_∞ is removed. $B(w)$ is an even, real and positive function.

Using (1), (2), the motion response of the WEC system is given by

$$V(jw) = \frac{1}{Z_i(jw)}\left[F_{ex}(jw) - F_u(jw)\right] \quad (3)$$

where

$$Z_i(jw) = B(w) + jw\left[M - \frac{K_{hd}}{w^2} + M_\infty + M_a(w)\right] \quad (4)$$

$Z_i(jw)$ is the intrinsic impedance of the system. Rewrite $Z_i(jw)$ as

$$Z_i(jw) = R_i(w) + jX_i(w) \quad (5)$$

with

$$\begin{cases} R_i(w) = B(w), \\ X_i(w) = w\left[M - \frac{K_{hd}}{w^2} + M_\infty + M_a(w)\right] \end{cases} \quad (6)$$

It is clear that $R_i(w)$ is an even, real and positive function.

C. Control Objective

The control objective is to select $f_u(t)$ that maximizes the extracted average power produced by the WEC

$$P_a = \frac{1}{T}\int_0^T f_u(t)v(t)dt \quad (7)$$

while respecting the following constraints on the PTO input $f_u(t)$, the WEC velocity $v(t)$, and the WEC position $s(t)$

$$\begin{cases} -F_{lim} \le f_u(t) \le F_{lim}, \\ -V_{lim} \le v(t) \le V_{lim}, \\ -S_{lim} \le s(t) \le S_{lim} \end{cases} \quad (8)$$

D. Earlier Works on Adaptive PI Control

If the PI control structure is selected, then $f_u(t)$ is given as

$$f_u(t) = K_p v(t) + K_i \int_0^t v(\tau)d\tau$$

where K_p, K_i are the PI gains. Assuming zero initial position, one has

$$f_u(t) = K_p v(t) + K_i s(t) \quad (9)$$

since $s(t) = \int_0^t v(\tau)d\tau$. In the frequency domain

$$F_u(jw) = \left(K_p + \frac{K_i}{jw}\right) V(jw) \tag{10}$$

In a monochromatic sea state, the wave excitation force is given as

$$f_{ex}(t) = A_0 \sin(w_0 t + \phi_0) \tag{11}$$

where A_0, w_0, ϕ_0 are, respectively, the amplitude, the angular wave frequency, and the phase.

For a given $f_{ex}(t)$ in (11), and without the constraints (8), it was shown in the complex conjugate control theory [3], [4] that P_a attains the maximum when the PTO input is given as

$$F_u(jw_0) = (R_i(w_0) - jX_i(w_0))\, V(jw_0) \tag{12}$$

where $R_i(w_0), X_i(w_0)$ are given in (6) with $w = w_0$.

Using (10), (12), one obtains

$$\begin{cases} K_p = R_i(w_0), \\ K_i = w_0 X_i(w_0) \end{cases} \tag{13}$$

under the monochromatic sea state assumption (11).

There are two problems for the implementation of the control law (9), (13). The first one is that real sea states are polychromatic, i.e., $f_{ex}(t)$ is not a pure sinusoid. The second problem is that $f_{ex}(t)$ cannot be measured directly when the WEC system is running.

To address the polychromatic sea state problem, in [13], [16], the real wave excitation force is modeled as a time-varying sinusoidal signal, i.e.,

$$f_{ex}(t) = A_0(t) \sin(w_0(t)t + \phi_0(t)) \tag{14}$$

where the parameters $A_0(t), w_0(t)$ and $\phi_0(t)$ are estimated online. Since $f_{ex}(t)$ is a nonlinear function of $A_0(t), w_0(t), \phi_0(t)$, the estimation problem is nonlinear. A possible solution to the problem is to employ an unscented Kalman filter (UKF) [17]. The main advantage of the UKF is that it is already evaluated experimentally on real wave data [16] with a good performance.

To address the problem that $f_{ex}(t)$ is not directly measurable, the concept of soft sensor can be used. The basic idea is to combine the WEC mathematical model (3) with available measurements such as $f_u(t), v(t), s(t)$ for estimating $f_{ex}(t)$. A possible solution to this problem is to use a linear Kalman filter (LKF) [12]. It was shown experimentally in [12] that LKF produces accurate estimates over a large range of sea states.

The adaptive PI control strategy is summarized in Algorithm 1.

Algorithm 1: Adaptive PI Control

1: At each time instant t.
2: Estimate $\hat{f}_{ex}(t)$ using an LKF.
3: Estimate $\hat{w}_0(t)$ using an UKF.
4: Compute the gains K_p, K_i using (13).
5: Compute the control action $f_u(t)$ using (9).

The adaptive PI control algorithm is schematically presented in Fig. 2. This control law is obtained without considering the constraints (8). Hence, a saturation block is placed at the output of the PI control law in order to cope with the input constraints, see Fig. 2. Note that the position and velocity constraints are not taken into account in this control strategy.

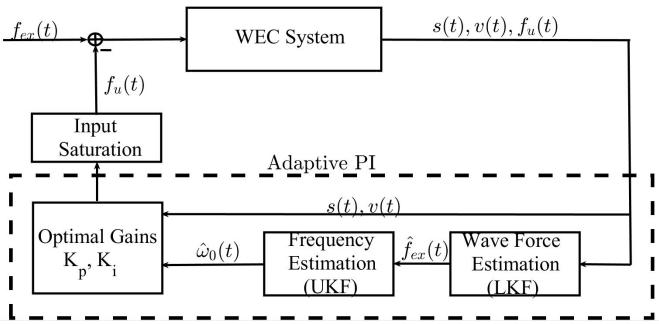

Fig. 2: Schematic diagram of adaptive PI control.

III. Constrained Adaptive PI Control

In this section we propose a new adaptive PI control strategy. Its main distinguished feature is that the force and motions constraints are taken into consideration in the design phase.

A. Optimal Control in Regular Waves

Following [3], [4], the PTO input is assumed to be a linear function of the velocity, i.e.,

$$F_u(jw) = Z_c(jw)V(jw) \tag{15}$$

where $Z_c(jw)$ is a design variable.

Using (3), (15), one obtains

$$V(jw) = \frac{1}{Z_i(jw)}(F_{ex}(jw) - Z_c(jw)V(jw)) \tag{16}$$

or, equivalently

$$V(jw) = \frac{1}{Z_i(jw) + Z_c(jw)} F_{ex}(jw) = G(jw)F_{ex}(jw) \tag{17}$$

$G(jw)$ is the closed-loop transfer function with the input $F_{ex}(jw)$, and with the output $V(jw)$

$$G(jw) = \frac{1}{Z_i(jw) + Z_c(jw)} \tag{18}$$

$G(jw)$ is a complex number. It can be decomposed as

$$G(jw) = R_g(w) + jX_g(w) \tag{19}$$

where $R_g(w), X_g(w)$ are the real part and the imaginary part of $G(jw)$, respectively.

For simplicity, the arguments w, w_0 will be omitted whenever possible. The following theorem holds.

Theorem 1: Given the wave excitation force (11) and the PTO input (15), the average power is computed as

$$P_a = \frac{A_0^2}{2}\left[R_g(w_0) - R_i(w_0)R_g(w_0)^2 - R_i(w_0)X_g(w_0)^2\right] \tag{20}$$

Proof: See Appendix A. □

Theorem 1 gives an analytical expression of the average power in terms of the hydrodynamic coefficients. Concerning the constraints (8), define $A_i(w_0) = \sqrt{R_i(w_0)^2 + X_i(w_0)^2}$, i.e., $A_i(w_0)$ is the magnitude of $Z_i(jw_0)$. The following theorem holds

Theorem 2: Given the wave excitation force (11) and the PTO input (15), the constraints (8) are satisfied if and only if

- For the input constraint

$$\left(R_g - \frac{R_i}{A_i^2}\right)^2 + \left(X_g + \frac{X_i}{A_i^2}\right)^2 \leq \frac{F_{lim}^2}{A_0^2 A_i^2} \tag{21}$$

- For the velocity constraint

$$R_g^2 + X_g^2 \leq \frac{V_{lim}^2}{A_0^2} \tag{22}$$

- For the position constraint

$$R_g^2 + X_g^2 \leq \frac{w_0^2 S_{lim}^2}{A_0^2} \tag{23}$$

Proof: See Appendix B. □

Using Theorem 1 and Theorem 2, one can rewrite the problem of maximizing the harvested average power subject to the constraints (8) as

$$\max_{R_g, X_g} \left\{ \tfrac{A_0^2}{2} \left[R_g - R_i R_g^2 - R_i X_g^2 \right] \right\}, \quad \text{s.t.} \begin{cases} \left(R_g - \frac{R_i}{A_i^2}\right)^2 + \left(X_g + \frac{X_i}{A_i^2}\right)^2 \leq \frac{F_{lim}^2}{A_0^2 A_i^2}, \\ R_g^2 + X_g^2 \leq \frac{V_{lim}^2}{A_0^2}, \\ R_g^2 + X_g^2 \leq \frac{w_0^2 S_{lim}^2}{A_0^2} \end{cases} \tag{24}$$

Since $R_i = B(w_0)$ is positive, (24) can be rewritten as

$$\min_{R_g, X_g} \left\{ \left(R_g - \tfrac{1}{2R_i}\right)^2 + X_g^2 \right\}, \quad \text{s.t.} \begin{cases} \left(R_g - \frac{R_i}{A_i^2}\right)^2 + \left(X_g + \frac{X_i}{A_i^2}\right)^2 \leq \frac{F_{lim}^2}{A_0^2 A_i^2}, \\ R_g^2 + X_g^2 \leq \frac{V_{lim}^2}{A_0^2}, \\ R_g^2 + X_g^2 \leq \frac{w_0^2 S_{lim}^2}{A_0^2} \end{cases} \tag{25}$$

Define

$$\xi_1 = R_g - \frac{1}{2R_i},\ \xi_2 = X_g,\ \xi = [\xi_1 \ \ \xi_2]^T \tag{26}$$

Using (26), one can rewrite problem (25) as

$$\min_{\xi} \left\{ \xi_1^2 + \xi_2^2 \right\} \tag{27}$$

$$\text{s.t. } \left(\xi_1 + \frac{1}{2R_i} - \frac{R_i}{A_i^2}\right)^2 + \left(\xi_2 + \frac{X_i}{A_i^2}\right)^2 \leq \frac{F_{lim}^2}{A_0^2 A_i^2}, \tag{28}$$

$$\left(\xi_1 + \frac{1}{2R_i}\right)^2 + \xi_2^2 \leq \frac{V_{lim}^2}{A_0^2}, \tag{29}$$

$$\left(\xi_1 + \frac{1}{2R_i}\right)^2 + \xi_2^2 \leq \frac{w_0^2 S_{lim}^2}{A_0^2} \tag{30}$$

The solution ξ^* to (27), (28), (29), (30) is unique because the cost and the constraints are convex. ξ^* can be found by using any numerical procedure for convex optimization. Here we show how to obtain a closed-form for ξ^*.

It is clear that if $\frac{V_{lim}^2}{A_0^2} \leq \frac{w_0^2 S_{lim}^2}{A_0^2}$ then the constraint (30) is redundant. Otherwise, (29) is redundant. For simplicity, only the position constraint (30) is considered in the rest of the paper. Define

$$\begin{cases} a^* = -\left(1 - \frac{F_{lim}}{A_0 A_i \sqrt{\left(\frac{1}{2R_i} - \frac{R_i}{A_i^2}\right)^2 + \frac{X_i^2}{A_i^4}}}\right) \begin{bmatrix} \frac{1}{2R_i} - \frac{R_i}{A_i^2} \\ \frac{X_i}{A_i^2} \end{bmatrix}, \\ b^* = -\begin{bmatrix} \frac{1}{2R_i} - \frac{w_0 S_{lim}}{A_0} \\ 0 \end{bmatrix}, \\ c^* = -\begin{bmatrix} \frac{X_i^2}{R_i A_i^2}\alpha + \frac{1}{2A_0^2 R_i}(F_{lim}^2 - w_0^2 S_{lim}^2 A_i^2) \\ \frac{X_i}{A_i^2}\alpha \end{bmatrix} \end{cases} \tag{31}$$

where

$$\begin{cases} \zeta = A_0^2 + w_0^2 S_{lim}^2 A_i^2 - F_{lim}^2, \\ \alpha = \frac{1}{2A_0^2}\zeta + \frac{A_i R_i}{A_0 X_i}\sqrt{w_0^2 S_{lim}^2 - \frac{\zeta^2}{4A_0^2 A_i^2}} \end{cases} \tag{32}$$

The following theorem holds.

Theorem 3: Under the feasibility assumption, the solution of the following convex optimization problem

$$\min_{\xi} \left\{ \xi_1^2 + \xi_2^2 \right\} \tag{33}$$

$$\text{s.t. } \left(\xi_1 + \frac{1}{2R_i} - \frac{R_i}{A_i^2}\right)^2 + \left(\xi_2 + \frac{X_i}{A_i^2}\right)^2 \leq \frac{F_{lim}^2}{A_0^2 A_i^2}, \tag{34}$$

$$\left(\xi_1 + \frac{1}{2R_i}\right)^2 + \xi_2^2 \leq \frac{w_0^2 S_{lim}^2}{A_0^2} \tag{35}$$

is given by,

$$\begin{cases} \xi^* = \begin{bmatrix} 0 \\ 0 \end{bmatrix}, \text{ if } & \begin{cases} \left(\frac{1}{2R_i} - \frac{R_i}{A_i^2}\right)^2 + \left(\frac{X_i}{A_i^2}\right)^2 \leq \frac{F_{lim}^2}{A_0^2 A_i^2}, \\ \frac{1}{2R_i} \leq \frac{w_0 S_{lim}}{A_0} \end{cases} \\ \xi^* = a^*, \text{else-if} & \begin{cases} \left(\frac{1}{2R_i} - \frac{R_i}{A_i^2}\right)^2 + \left(\frac{X_i}{A_i^2}\right)^2 \geq \frac{F_{lim}^2}{A_0^2 A_i^2}, \\ \left(a_1^* + \frac{1}{2R_i}\right)^2 + (a_2^*)^2 \leq \frac{w_0^2 S_{lim}^2}{A_0^2} \end{cases} \\ \xi^* = b^*, \text{else-if} & \begin{cases} \left(b_1^* + \frac{1}{2R_i} - \frac{R_i}{A_i^2}\right)^2 \\ \quad + \left(b_2^* + \frac{X_i}{A_i^2}\right)^2 \leq \frac{F_{lim}^2}{A_0^2 A_i^2}, \\ \frac{1}{2R_i} \geq \frac{w_0 S_{lim}}{A_0} \end{cases} \\ \xi^* = c^*, \text{otherwise} & \end{cases} \tag{36}$$

Proof: See Appendix C. □

Once the solution ξ^* of (33), (34), (35) is computed, using (26), one gets

$$R_g^* = \xi_1^* + \frac{1}{2R_i}, X_g^* = \xi_2^* \tag{37}$$

Using (18), one obtains

$$\begin{aligned} Z_c(jw) &= \tfrac{1}{G(jw)} - Z_i(jw) \\ &= \left(\tfrac{R_g(w)}{R_g(w)^2 + X_g(w)^2} - R_i(w)\right) \\ &\quad -j\left(\tfrac{X_g(w)}{R_g(w)^2 + X_g(w)^2} + X_i(w)\right) \end{aligned}$$

Thus, using (37), the optimal real part and imaginary part of the control block are computed as

$$\begin{cases} R_c^* = \frac{R_g^*}{(X_g^*)^2 + (R_g^*)^2} - R_i, \\ X_c^* = -\frac{X_g^*}{(X_g^*)^2 + (R_g^*)^2} - X_i \end{cases} \tag{38}$$

Remark 1: Consider the unconstrained case, i.e., there are no constraints on the PTO force and on the WEC position. In this case, the optimal solution of (33) is $\xi_1^* = \xi_2^* = 0$. Using (37), one obtains $R_g^* = \frac{1}{2R_i}, X_g^* = 0$. Using (38), one gets

$$R_c^* = R_i, X_c^* = -X_i \tag{39}$$

Condition (39) is known as complex conjugate control. It was obtained in [3], [4]. Therefore the result in [3], [4] is a special case of Theorem 3. □

Remark 2: The results in this section answer only the question of how to maximize the harvested power in the nominal case with force and motions constraints. We do not take into consideration the model uncertainties in this work.

B. Feasibility Analysis

We study the feasibility problem of (33), (34), (35) in this section. In other words, we would like to know under what conditions for F_{lim}, S_{lim}, problem (33), (34), (35) has a solution for a given wave excitation force (11).

The constraints (34), (35) describe two circles of radius $\frac{F_{lim}}{A_0 A_i}$, $\frac{w_0 S_{lim}}{A_0}$, respectively. Fig. 3 presents the two sets. The solid blue line describes the PTO force constraint (34). The dashed red line describes the WEC position constraint (35). The intersection of the two circles is the feasible set.

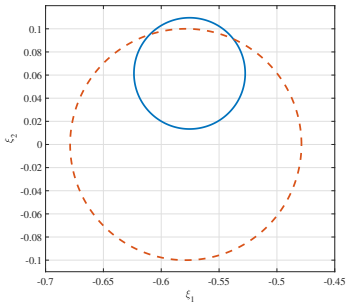

Fig. 3: Feasible set.

The following theorem holds.

Theorem 4: For a given wave excitation force (11), problem (33), (34), (35) is feasible if and only if

$$w_0 A_i S_{lim} + F_{lim} \geq A_0 \tag{40}$$

Proof: See Appendix D. □

In a case, e.g., the amplitude A_0 of the wave excitation force is too large, condition (40) is not satisfied. This implies that there exists no linear control law with the given constrained PTO force $[-F_{lim},\ F_{lim}]$, that can keep the WEC position inside the constraints $[-S_{lim},\ S_{lim}]$.

The force constraints present physical limitations of the PTO actuator. They cannot be exceeded. In other words, F_{lim} is given and cannot be changed. On the other hand, the WEC position constraints are generally considered for safety reason. It is desirable to keep the WEC position inside the limits. However, violation can be tolerated for short time periods, e.g., when the wave excitation force is too large. In other words, S_{lim} can be modified if condition (40) is not satisfied.

In this paper, if the problem (33), (34), (35) is infeasible, then the WEC position upper bound is modified as

$$S_{lim} = \frac{A_0 - F_{lim}}{w_0 A_i} \tag{41}$$

In this case, using the proof of Theorem 4, the two circles touch at the point

$$\begin{cases} \xi_1^* = -\frac{1}{2R_i} + \frac{(A_0 - F_{lim})R_i}{A_0 A_i^2}, \\ \xi_2^* = -\frac{(A_0 - F_{lim})X_i}{A_0 A_i^2} \end{cases} \tag{42}$$

Hence (42) is the solution of (33), (34), (35) with S_{lim} in (41).

C. Extension to Irregular Waves

In this section we show how to extend the results in Section III-A and in Section III-B to polychromatic sea states. The idea is the same as in the standard unconstrained adaptive PI control, i.e., by approximating online $f_{ex}(t)$ as

$$f_{ex}(t) = A_0(t) \sin\left(w_0(t)t + \phi_0(t)\right)$$

where $A_0(t), w_0(t), \phi_0(t)$ are time-varying. We use the LKF with information from $s(t), v(t)$ and $f_u(t)$ to estimate $f_{ex}(t)$. We then use the UKF to estimate $A_0(t), w_0(t)$.

If the PI structure is selected for the control block $Z_c(jw)$ then

$$Z_c(jw) = K_p + \frac{K_i}{jw}$$

Hence

$$K_p = R_c^*, K_i = -wX_c^* \tag{43}$$

where R_c^*, X_c^* are given in (38). Note that to calculate R_c^*, X_c^*, we need information both from the amplitude $A_0(t)$ and from the frequency $w_0(t)$. Recall that in the unconstrained adaptive PI control algorithm, only information from $w_0(t)$ is required.

The constrained adaptive PI control strategy is summarized in Algorithm 2.

Algorithm 2: Constrained Adaptive PI Control

1: At each time instant t.
2: Estimate $\hat{f}_{ex}(t)$ using an LKF.
3: Estimate $\hat{A}_0(t), \hat{w}_0(t)$ using an UKF.
4: If condition (40) holds, then calculate ξ^* using (36).
5: Otherwise, calculate ξ^* using (42).
6: Calculate R_g^*, X_g^* using (37).
7: Calculate R_c^*, X_c^* using (38).
8: Calculate K_i, K_p using (43).
9: The control action is computed as

$$f_u(t) = K_p v(t) + K_i s(t)$$

The constrained adaptive PI control algorithm is schematically presented in Fig. 4. In comparison with the standard unconstrained adaptive PI control strategy, see Fig. 2, the new one does not require the saturation block at its output. This is because the input constraints are taken into account in the design phase.

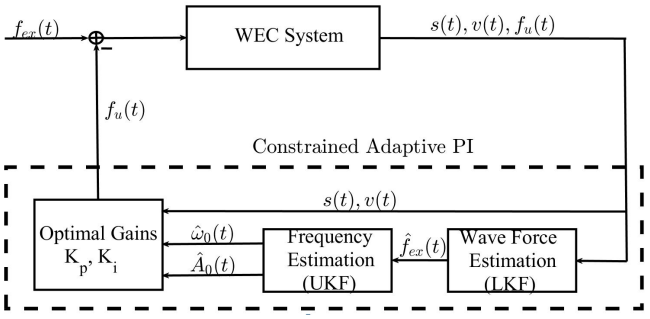

Fig. 4: Schematic diagram of constrained adaptive PI control structure.

D. Stability Analysis

In this section we analyze the stability of the closed-loop system (17) with the control law in Algorithm 2. Since the problem treated in the paper is to maximize the harvested power in (7), the notion of stability is understood in an *input-output* sense. That is, we say that the system is stable if bounded wave excitation force $f_{ex}(t)$ supplied to the system yields bounded speed $v(t)$.

The basic idea to prove the stability of (17) is to show that system (17) is passive, and therefore stable. For this purpose, the following lemma is recalled.

Lemma 1: [18] Consider the single-input single-output system $y_p(jw) = G_p(jw)u_p(jw)$, where y_p is the output, u_p is the input, and G_p is the transfer function. The system is passive if and only if $Re(G_p(jw)) > 0$ at all frequencies w.

It is well known [18] that the negative feedback interconnection of two passive systems yields a passive system. Using Fig. 4, the system (17) is consisted of two subsystems via the negative feedback: i) the WEC system; ii) the PI control law. It is well known [8] that the WEC system is passive. It remains to show that $Z_c(jw)$ is passive. Since the $P-$component converts the wave energy into useful energy, one must have $K_p > 0$. Hence $Re(Z_c(jw)) = K_p > 0$, or equivalently $Z_c(jw)$ is passive. It follows that the closed-loop system (17) is passive. Therefore, stability is guaranteed.

Remark 3: An alternative way to prove the passivity of $G(jw)$ is to show directly that $Re(G(jw)) > 0$. Note that $Re(G(jw)) = R_g$. Using the cost function in (24), one should have $R_g > 0$, because $R_i > 0$ and the harvested power P_a should be positive. Hence $G(jw)$ is a passive system.

IV. Simulation Results

A. WEC Parameters

To illustrate the effectiveness of the proposed control algorithm in Section III, we use a laboratory prototype of a point absorber WEC on a 1:20 scale with respect to the well-known Wavestar machine [23]. The motion is rotational for the Wavestar system. Hence the units of the PTO input, the position and the speed are Nm, rad and rad/s, respectively. The WEC parameters are $M = 1.44$, $K_{hd} = 93$, and

$$Z_r(jw) = \frac{a_3(jw)^3 + a_2(jw)^2 + a_1(jw) + a_0}{b_3(jw)^3 + b_2(jw)^2 + b_1(jw) + b_0} \qquad (44)$$

$\{a_3, \ldots, a_0, b_3, \ldots, b_0\}$ are given in Table I.

Numerator	Denominator
$a_3 = 0.000273$	$b_3 = 1$
$a_2 = 31.04$	$b_2 = 113.5$
$a_1 = 3421$	$b_1 = 1377$
$a_0 = -9.145$	$b_0 = 9061$

TABLE I: Radiation model parameters

The constraints are

$$-0.2 \le s(t) \le 0.2, \ -6.25 \le f_u(t) \le 6.25$$

In other words, $S_{lim} = 0.2$, $F_{lim} = 6.25$.

Using the results in Section III, Fig. 5 presents the optimal R_c, X_c of the control block, and the maximal harvested average power P_a as a function of w_0 and A_0 with $0.3 \le w_0 \le 12$, $0.1 \le A_0 \le 6$. Recall that in the unconstrained case, R_c and X_c depend uniquely on w_0.

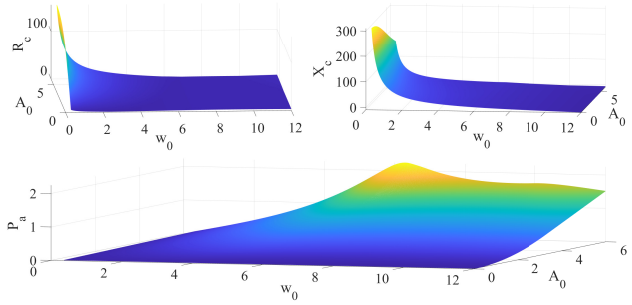

Fig. 5: Optimal real part and imaginary part of the control block and maximal harvested average power.

B. Simulation Results

In this section, we show the simulation results obtained using the constrained adaptive PI control algorithm. To validate our concept, we choose three sea states, that represent real life sea conditions for the Wavestar machine. The wave amplitudes increase, and the peak wave frequencies decrease from wave 1 to wave 3. The waves were generated by the wave maker of Aalborg University based on the Pierson-Moskowitz spectrum. Fig. 6 presents the power spectral density of the three waves.

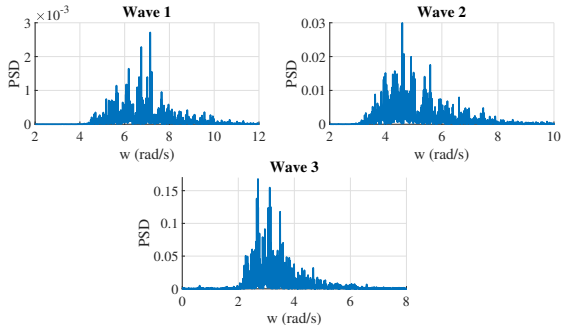

Fig. 6: Power spectral density of the waves.

In parallel with the new control law in Algorithm 2, we use the unconstrained adaptive PI control law in Algorithm 1 for comparison purpose.

Fig 7 presents the PTO force $f_u(t)$, the WEC position $s(t)$, the WEC velocity $v(t)$, and the harvested energy $E(t)$ for wave 1 using Algorithm 1 (dashed red line) and Algorithm 2 (solid blue line). $E(t)$ is calculated as $E(t) = \int_0^t f_u(\tau)v(\tau)d\tau$. Since the amplitudes of wave 1 are relatively small, the PTO force and the WEC position constraints are not hit. Hence it is expected that the performances of Algorithm 1, and of Algorithm 2 are identical. This can be observed in Fig 7.

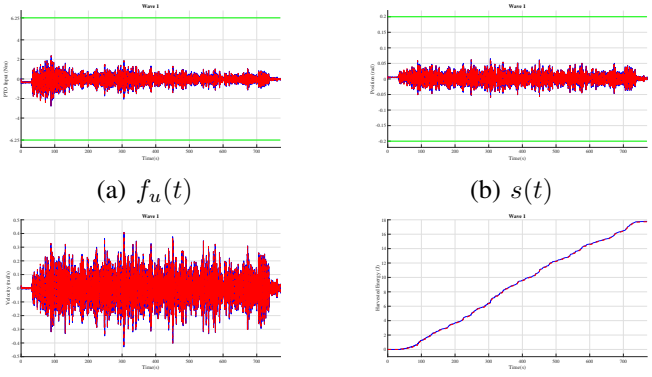

(a) $f_u(t)$ (b) $s(t)$

(c) $v(t)$ (d) $E(t)$

Fig. 7: Performance comparison between Algorithm 1 (dashed red line) and Algorithm 2 (solid blue line) for wave 1.

Fig. 8 shows $f_u(t), s(t), v(t)$, and $E(t)$ for wave 2 as a function of time using Algorithm 1 (dashed red line) and Algorithm 2 (solid blue line). Using Fig. 8, the following remarks can be made

- Using Fig. 8(a), $f_u(t)$ is often saturated. This is because the amplitudes of wave 2 are larger than that of wave 1.
- Using Fig. 8(b), the WEC position constraints are satisfied all the time with Algorithm 2, while this is not the case with Algorithm 1.
- Using Fig. 8(c), the WEC oscillates with much higher speed using Algorithm 1 than that using Algorithm 2. Consequently, the mechanical fatique of the WEC system is more important with Algorithm 1 than that with Algorithm 2.
- Using Fig. 8(d), Algorithm 2 harvests slightly more energy than Algorithm 1.

Fig. 9 presents the zoomed-in $f_u(t)$, $v(t)$ and $s(t)$ for the time interval $100(s) \leq t \leq 120(s)$ for wave 2.

Fig. 10 shows $f_u(t), s(t), v(t)$, and $E(t)$ for wave 3 as a function of time using Algorithm 1 (dashed red line) and Algorithm 2 (solid blue line). The amplitudes of wave 3 are largest among the three waves. Hence the PTO force is saturated much more often with wave 3 than with other waves, see Fig. 10(a). It can be observed using Fig. 10(d) that we gain 287% more energy with Algorithm 2 than with Algorithm 1.

Fig. 11 presents the zoomed-in $f_u(t)$, $v(t)$ and $s(t)$ for the time interval $1175(s) \leq t \leq 1200(s)$ for wave 3. As discussed in Section III, while the PTO force constraints cannot be modified, the WEC position constraints are tolerated to violate for short time periods. The violation of the constraints on

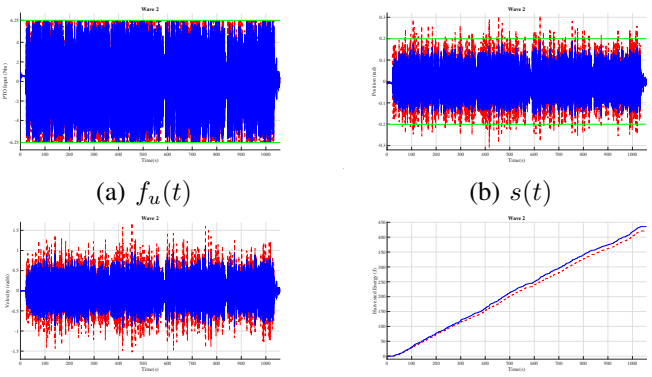

(a) $f_u(t)$ (b) $s(t)$

(c) $v(t)$ (d) $E(t)$

Fig. 8: Performance comparison between Algorithm 1 (dashed red line) and Algorithm 2 (solid blue line) for wave 2.

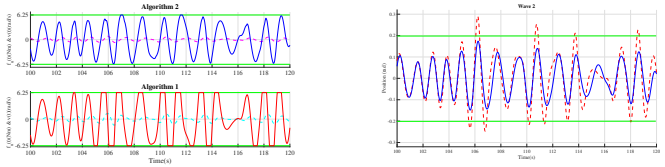

Fig. 9: Zoomed-in: $f_u(t)$-Algorithm 2 (solid blue), $v(t)$-Algorithm 2 (dashed magenta), $f_u(t)$-Algorithm 1 (solid red), $v(t)$-Algorithm 1 (dashed cyan), $s(t)-$Algorithm 2 (solid blue), $s(t)-$Algorithm 1 (dashed red) for wave 2.

$s(t)$ for Algorithm 2 can be observed in Fig. 11 at time $t \approx 1186[sec]$.

V. Conclusion

In this paper we propose a new adaptive PI control strategy to the problem of maximizing the harvested energy with a point absorber under the force and motion constraints. First, regular waves were considered where the problem of maximizing the harvested power can be reformulated as a convex optimization problem. We show how to obtain a closed-form solution for this problem. We also show the relationship

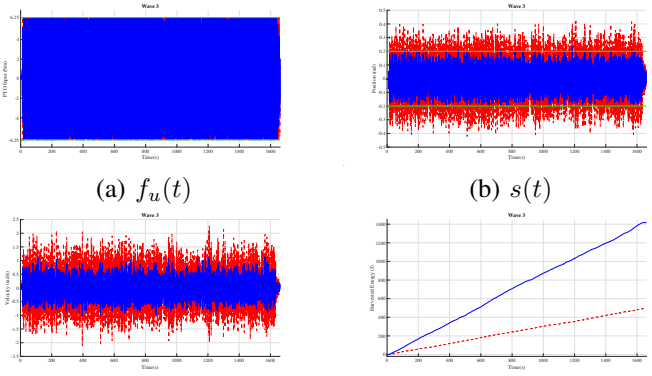

(a) $f_u(t)$ (b) $s(t)$

(c) $v(t)$ (d) $E(t)$

Fig. 10: Performance comparison for Algorithm 1 (dashed red line) and Algorithm 2 (solid blue line) for wave 3.

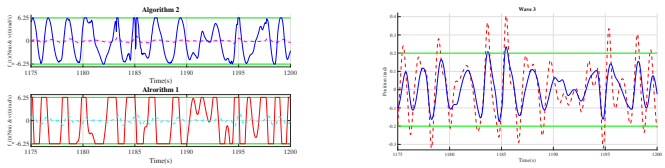

Fig. 11: Zoomed-in: $f_u(t)$-Algorithm 2 (solid blue), $v(t)$-Algorithm 2 (dashed magenta), $f_u(t)$-Algorithm 1 (solid red), $v(t)$-Algorithm 1 (dashed cyan), $s(t)-$Algorithm 2 (solid blue), $s(t)-$Algorithm 1 (dashed red) for wave 3.

between the wave amplitude, the wave frequency and the constraints in order to guarantee the feasibility of the optimization problem. Then, by approximating the real irregular wave as a time-varying sinusoid, the new control law is proposed. The gains of the new control law are continuously adapted on-line on a wave-to-wave basis. A simulation example is given and compared to an earlier solution from literature.

In the future we will extend the proposed technique to the case of wave energy converter with uncertain dynamics. We will also study other types of wave energy converter, and the multi-float configuration case.

REFERENCES

[1] Aurélien Babarit and Alain H Clément. Optimal latching control of a wave energy device in regular and irregular waves. *Applied Ocean Research*, 28(2):77–91, 2006.

[2] Julien AM Cretel, Anthony W Lewis, Gareth P Thomas, and Gordon Lightbody. A critical assessment of latching as control strategy for wave-energy point absorbers. In *The Twenty-first International Offshore and Polar Engineering Conference*. OnePetro, 2011.

[3] DV Evans. Power from water waves. *Annual review of Fluid mechanics*, 13(1):157–187, 1981.

[4] Johannes Falnes. *Ocean waves and oscillating systems: linear interactions including wave-energy extraction*. Cambridge university press, 2002.

[5] Francesco Fusco and John V Ringwood. A simple and effective real-time controller for wave energy converters. *IEEE Transactions on sustainable energy*, 4(1):21–30, 2012.

[6] Demián García-Violini, Yerai Peña-Sanchez, Nicolás Faedo, Francesco Ferri, and John V Ringwood. A broadband time-varying energy maximising control for wave energy systems (lite-con+): Framework and experimental assessment. *IEEE Transactions on Sustainable Energy*, 2023.

[7] Jørgen Hals, Johannes Falnes, and Torgeir Moan. A comparison of selected strategies for adaptive control of wave energy converters. *Journal of Offshore Mechanics and Arctic Engineering*, 133(3):031101, 2011.

[8] Alyssa Kody, Nathan Tom, and Jeffrey Scruggs. Model predictive control of a wave energy converter using duality techniques. In *2019 American Control Conference (ACC)*, pages 5444–5451. IEEE, 2019.

[9] UA Korde. Efficient primary energy conversion in irregular waves. *Ocean engineering*, 26(7):625–651, 1999.

[10] UA Korde, MP Schoen, and F Lin. Time domain control of a single mode wave energy device. In *The Eleventh International Offshore and Polar Engineering Conference*. OnePetro, 2001.

[11] Guang Li and Michael R Belmont. Model predictive control of sea wave energy converters–part i: A convex approach for the case of a single device. *Renewable Energy*, 69:453–463, 2014.

[12] H-N Nguyen and Paolino Tona. Wave excitation force estimation for wave energy converters of the point-absorber type. *IEEE Transactions on Control Systems Technology*, 26(6):2173–2181, 2017.

[13] Hoai-Nam Nguyen. Robust adaptive pi control of wave energy converters with uncertain dynamics. *IFAC Journal of Systems and Control*, 19:100183, 2022.

[14] Hoai Nam Nguyen. Is the velocity always in phase with the wave excitation force in constrained optimal control of wave energy converters? In *IFAC WC 2023*, 2023.

[15] Hoai-Nam Nguyen, Guillaume Sabiron, Paolino Tona, Morten Mejlhede Kramer, and Enrique Vidal Sanchez. Experimental validation of a nonlinear mpc strategy for a wave energy converter prototype. In *International Conference on Offshore Mechanics and Arctic Engineering*, volume 49972, page V006T09A019. American Society of Mechanical Engineers, 2016.

[16] Hoai-Nam Nguyen and Paolino Tona. An efficiency-aware continuous adaptive proportional-integral velocity-feedback control for wave energy converters. *Renewable Energy*, 146:1596–1608, 2020.

[17] Hoai-Nam Nguyen, Paolino Tona, and Guillaume Sabiron. Dominant wave frequency and amplitude estimation for adaptive control of wave energy converters. In *OCEANS 2017-aberdeen*, pages 1–6. IEEE, 2017.

[18] Romeo Ortega, Julio Antonio Loría Perez, Per Johan Nicklasson, and Hebertt J Sira-Ramirez. *Passivity-based control of Euler-Lagrange systems: mechanical, electrical and electromechanical applications*. Springer Science & Business Media, 2013.

[19] Markus Richter, Mario E Magana, Oliver Sawodny, and Ted KA Brekken. Nonlinear model predictive control of a point absorber wave energy converter. *IEEE Transactions on Sustainable Energy*, 4(1):118–126, 2012.

[20] Enrique Vidal Sánchez, Rico Hjerm Hansen, and Morten Mejlhede Kramer. Control performance assessment and design of optimal control to harvest ocean energy. *IEEE Journal of Oceanic Engineering*, 40(1):15–26, 2015.

[21] Jiajun Song, Ossama Abdelkhalik, Rush Robinett, Giorgio Bacelli, David Wilson, and Umesh Korde. Multi-resonant feedback control of heave wave energy converters. *Ocean Engineering*, 127:269–278, 2016.

[22] Siyuan Zhan, Peter Stansby, Zhijing Liao, and Guang Li. A fast model predictive control framework for multi-float and multi-mode-motion wave energy converters. *IEEE Transactions on Control Systems Technology*, 2022.

[23] Andrew S Zurkinden, Morten Kramer, Mahdi Teimouri Teimouri, and Marco Alves. Comparison between numerical modeling and experimental testing of a point absorber wec using linear power take-off system. In *ASME 2012 31st International Conference on Ocean, Offshore and Arctic Engineering*, pages 497–506. American Society of Mechanical Engineers, 2012.

APPENDIX

Appendix A. (Proof of Theorem 1): Using (15), (18), one obtains

$$F_u(jw) = \left(\frac{1}{G(jw)} - Z_i(jw)\right) V(jw)$$

thus, with (17)

$$F_u(jw) = \left(1 - Z_i(jw)G(jw)\right) F_{ex}(jw) \tag{45}$$

Without loss of generality, the phase ϕ_0 of $f_{ex}(t)$ in (11) can be set to be zero. Because (45) is a linear system, one obtains, for $f_{ex}(t)$ given in (11)

$$f_u(t) = A_u A_0 \sin(w_0 t + \theta_u) \tag{46}$$

where A_u and θ_u are, respectively, the magnitude and the phase of $(1 - Z_i(jw)G(jw))$, evaluated at frequency w_0, i.e.,

$$\begin{cases} A_u = |1 - Z_i(jw_0)G(jw_0)|, \\ \theta_u = \angle\left(1 - Z_i(jw_0)G(jw_0)\right) \end{cases}$$

Similarly, because (17) is a linear system, one gets

$$v(t) = A_g A_0 \sin(w_0 t + \theta_g) \tag{47}$$

where $A_g = |G(jw_0)|$ and $\theta_g = \angle G(jw_0)$ are, respectively, the magnitude and the phase of $G(jw)$ evaluated at w_0.

Combining (46), (47), one gets

$$\begin{aligned} P_a &= \tfrac{1}{T}\int_0^T v(t) f_u(t) dt \\ &= \tfrac{1}{T}\int_0^T A_g A_u A_0^2 \sin(w_0 t + \theta_g)\sin(w_0 t + \theta_u) dt \end{aligned} \tag{48}$$

Since the wave excitation force (11) is periodic, it is clear that it suffices to calculate P_a for one period $T = \frac{2\pi}{w_0}$. Therefore

$$P_a = \frac{w_0}{2\pi} A_g A_u A_0^2 \int_0^{\frac{2\pi}{w_0}} \sin(w_0 t + \theta_g) \sin(w_0 t + \theta_u) dt \quad (49)$$

Using the following trigonometric identity

$$\sin(\alpha)\sin(\beta) = \frac{1}{2}[\cos(\alpha - \beta) - \cos(\alpha + \beta)]$$

one obtains from (49)

$$P_a = \frac{w_0}{4\pi} A_g A_u A_0^2 \left[\int_0^{\frac{2\pi}{w_0}} \cos(\theta_g - \theta_u) dt - \int_0^{\frac{2\pi}{w_0}} \cos(2w_0 t + \theta_g + \theta_u) dt \right]$$
$$= \frac{w_0}{4\pi} A_g A_u A_0^2 \left[\cos(\theta_g - \theta_u) t - \frac{\sin(2w_0 t + \theta_g + \theta_u)}{2w_0} \right] \Big|_0^{\frac{2\pi}{w_0}}$$

It follows

$$P_a = \frac{1}{2} A_g A_u A^2 \cos(\theta_g - \theta_u) \quad (50)$$

Using the following product-to-sum trigonometric identity

$$\cos(\theta_g - \theta_u) = \cos(\theta_g)\cos(\theta_u) + \sin(\theta_g)\sin(\theta_u)$$

one obtains, from (50)

$$P_a = \tfrac{1}{2} A_g A_u A^2 \left[\cos(\theta_g)\cos(\theta_u) + \sin(\theta_g)\sin(\theta_u)\right] \quad (51)$$

The following equations hold, see Fig. 12

$$\begin{cases} A_g \cos(\theta_g) = R_g, \\ A_g \sin(\theta_g) = X_g, \\ A_u \cos(\theta_u) = 1 - R_i R_g + X_i X_g, \\ A_u \sin(\theta_u) = -R_i X_g - X_i R_g \end{cases} \quad (52)$$

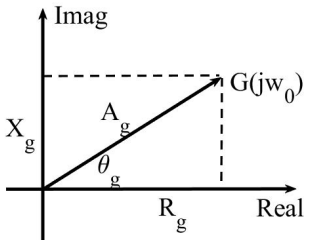

Fig. 12: Graphical illustration for equation (52).

Hence, using (51), one obtains

$$P_a = \frac{A^2}{2}\left[R_g(1 - R_i R_g + X_i X_g) - X_g(R_i X_g + X_i R_g)\right]$$

or equivalently $P_a = \frac{A^2}{2}\left[R_g - R_i R_g^2 - R_i X_g^2\right]$. The proof is complete. □

Appendix B. (Proof of Theorem 2): Concerning the input constraint (8), using (46), (52), one gets

$$f_u(t) = A_u A_0 \sin(w_0 t + \theta_u)$$
$$= \sqrt{(1 - R_i R_g + X_i X_g)^2 + (R_i X_g + X_i R_g)^2} A_0 \sin(w_0 t + \theta_u)$$

Hence $-F_{lim} \le f_u(t) \le F_{lim}$ if and only if

$$(1 - R_i R_g + X_i X_g)^2 + (R_i X_g + X_i R_g)^2 \le \frac{F_{lim}^2}{A_0^2}$$

or equivalently

$$\left(R_g - \frac{R_i}{R_i^2 + X_i^2}\right)^2 + \left(X_g + \frac{X_i}{R_i^2 + X_i^2}\right)^2 \le \frac{F_{lim}^2}{A_0^2 (R_i^2 + X_i^2)}$$

since $A_i = \sqrt{R_i^2 + X_i^2}$, one gets

$$\left(R_g - \frac{R_i}{A_i^2}\right)^2 + \left(X_g + \frac{X_i}{A_i^2}\right)^2 \le \frac{F_{lim}^2}{A_0^2 A_i^2}$$

Concerning the velocity constraint (8), using (47), (52), one obtains

$$v(t) = A_g A_0 \sin(w_0 t + \theta_g) = \sqrt{R_g^2 + X_g^2} A_0 \sin(w_0 t + \theta_g)$$

Hence the velocity constraint is satisfied if and only if

$$R_g^2 + X_g^2 \le \frac{V_{lim}^2}{A_0^2}$$

Concerning the position constraint, note that $S(jw) = \frac{1}{jw} V(jw)$. Thus, with (17), $S(jw) = \frac{G(jw)}{jw} F_{ex}(jw)$. For the given wave excitation force (11), one gets

$$\begin{aligned} s(t) &= \tfrac{A_g}{w_0} A_0 \sin(w_0 t + \theta_g - \tfrac{\pi}{2}) \\ &= \tfrac{\sqrt{R_g^2 + X_g^2}}{w_0} A_0 \sin(w_0 t + \theta_g - \tfrac{\pi}{2}) \end{aligned}$$

It follows that the position constraint is satisfied if and only if

$$R_g^2 + X_g^2 \le \frac{w_0^2 S_{lim}^2}{A_0^2} \quad (53)$$

The proof is complete. □

Appendix C. (Proof of Theorem 3): The Lagrangian $\mathcal{L}(\cdot)$ of (33), (34), (35) is given by

$$\begin{aligned} \mathcal{L}(\xi, \lambda) = {} & \xi_1^2 + \xi_2^2 \\ & + \lambda_1 \left[\left(\xi_1 + \tfrac{1}{2R_i} - \tfrac{R_i}{A_i^2}\right)^2 + \left(\xi_2 + \tfrac{X_i}{A_i^2}\right)^2 - \tfrac{F_{lim}^2}{A_0^2 A_i^2} \right] \\ & + \lambda_2 \left[\left(\xi_1 + \tfrac{1}{2R_i}\right)^2 + \xi_2^2 - \tfrac{w_0^2 S_{lim}^2}{A_0^2} \right] \end{aligned} \quad (54)$$

where $\lambda_1 \ge 0$, $\lambda_2 \ge 0$ are the dual variables for the constraints (34), (35). Using Karush-Kuhn-Tucker conditions, the optimal solution satisfies $\lambda_1^* \ge 0, \lambda_2^* \ge 0$, and

- Stationary condition

$$\begin{cases} \frac{\partial \mathcal{L}}{\partial \xi_1} = 0, \\ \frac{\partial \mathcal{L}}{\partial \xi_2} = 0 \end{cases} \quad (55)$$

- Complementary slackness condition

$$\begin{cases} \lambda_1^* \left[\left(\xi_1^* + \tfrac{1}{2R_i} - \tfrac{R_i}{A_i^2}\right)^2 + \left(\xi_2^* + \tfrac{X_i}{A_i^2}\right)^2 - \tfrac{F_{lim}^2}{A_0^2 A_i^2} \right] = 0, \\ \lambda_2^* \left[\left(\xi_1^* + \tfrac{1}{2R_i}\right)^2 + (\xi_2^*)^2 - \tfrac{w_0^2 S_{lim}^2}{A_0^2} \right] = 0 \end{cases} \quad (56)$$

Using (55), one obtains

$$\begin{cases} \xi_1^* + \lambda_1^* \left(\xi_1^* + \tfrac{1}{2R_i} - \tfrac{R_i}{A_i^2}\right) + \lambda_2^* \left(\xi_1^* + \tfrac{1}{2R_i}\right) = 0, \\ \xi_2^* + \lambda_1^* \left(\xi_2^* + \tfrac{X_i}{A_i^2}\right) + \lambda_2^* \xi_2^* = 0 \end{cases}$$

or, equivalently

$$\begin{cases} \xi_1^* = \frac{-1}{1 + \lambda_1^* + \lambda_2^*} \left[\lambda_1^* \left(\tfrac{1}{2R_i} - \tfrac{R_i}{A_i^2}\right) + \tfrac{\lambda_2^*}{2R_i} \right], \\ \xi_2^* = \frac{-1}{1 + \lambda_1^* + \lambda_2^*} \tfrac{\lambda_1^* X_i}{A_i^2}, \end{cases} \quad (57)$$

There are four cases.

Case 1: The constraints (34), (35) are inactive. In this case $\lambda_1^* = \lambda_2^* = 0$. Using (57), one gets $\xi_1^* = 0, \xi_2^* = 0$. Note that (34), (35) are inactive if and only if

$$\begin{cases} \left(\frac{1}{2R_i} - \frac{R_i}{A_i^2}\right)^2 + \left(\frac{X_i}{A_i^2}\right)^2 \leq \frac{F_{lim}^2}{A_0^2 A_i^2}, \\ \frac{1}{2R_i} \leq \frac{w_0 S_{lim}}{A_0} \end{cases}$$

Case 2: (34) is active, (35) is inactive. In this case, $\lambda_1^* > 0, \lambda_2^* = 0$, and

$$\begin{cases} \xi_1^* = \frac{-\lambda_1^*}{1+\lambda_1^*}\left(\frac{1}{2R_i} - \frac{R_i}{A_i^2}\right), \\ \xi_2^* = \frac{-\lambda_1^*}{1+\lambda_1^*}\frac{X_i}{A_i^2}, \\ \left(\xi_1^* + \frac{1}{2R_i} - \frac{R_i}{A_i^2}\right)^2 + \left(\xi_2^* + \frac{X_i}{A_i^2}\right)^2 = \frac{F_{lim}^2}{A_0^2 A_i^2} \end{cases}$$

Solving this system of equations, one obtains $\xi_1^* = a_1^*, \xi_2^* = a_2^*$. We have case 2 if and only if

$$\begin{cases} \left(\frac{1}{2R_i} - \frac{R_i}{A_i^2}\right)^2 + \left(\frac{X_i}{A_i^2}\right)^2 \geq \frac{F_{lim}^2}{A_0^2 A_i^2}, \\ \left(a_1^* + \frac{1}{2R_i}\right)^2 + (a_2^*)^2 \leq \frac{w_0^2 S_{lim}^2}{A_0^2} \end{cases}$$

Case 3: (34) is inactive, (35) is active. In this case, $\lambda_1^* = 0, \lambda_2^* > 0$, and

$$\begin{cases} \xi_1^* = \frac{-\lambda_2^*}{1+\lambda_2^*}\frac{1}{2R_i}, \\ \xi_2^* = 0, \\ \left(\xi_1^* + \frac{1}{2R_i}\right)^2 + (\xi_2^*)^2 = \frac{w_0^2 S_{lim}^2}{A_0^2} \end{cases}$$

Solving this system of equations, one gets $\xi_1^* = b_1^*, \xi_2^* = b_2^*$. We have case 3 if and only if

$$\begin{cases} \left(b_1^* + \frac{1}{2R_i} - \frac{R_i}{A_i^2}\right)^2 + \left(b_2^* + \frac{X_i}{A_i^2}\right)^2 \leq \frac{F_{lim}^2}{A_0^2 A_i^2}, \\ \frac{1}{2R_i} \geq \frac{w_0 S_{lim}}{A_0} \end{cases}$$

Case 4: (34) and (35) are active. In this case, $\lambda_1^* > 0, \lambda_2^* > 0$, and

$$\begin{cases} \xi_1^* = -\alpha_1\left(\frac{1}{2R_i} - \frac{R_i}{A_i^2}\right) - \frac{\alpha_2}{2R_i}, \\ \xi_2^* = -\alpha_1\frac{X_i}{A_i^2}, \\ \left(\xi_1^* + \frac{1}{2R_i} - \frac{R_i}{A_i^2}\right)^2 + \left(\xi_2^* + \frac{X_i}{A_i^2}\right)^2 = \frac{F_{lim}^2}{A_0^2 A_i^2}, \\ \left(\xi_1^* + \frac{1}{2R_i}\right)^2 + (\xi_2^*)^2 = \frac{w_0^2 S_{lim}^2}{A_0^2} \end{cases} \tag{58}$$

where $\alpha_1 = \frac{\lambda_1^*}{1+\lambda_1^*+\lambda_2^*}, \alpha_2 = \frac{\lambda_2^*}{1+\lambda_1^*+\lambda_2^*}$. Since $\lambda_1^* \geq 0$, $\lambda_2^* \geq 0$, one has $0 \leq \alpha_1 < 1$, $0 \leq \alpha_2 < 1$.

By substituting the fourth equation of (58) into the third equation, one can rewrite (58) as

$$\begin{cases} \xi_1^* = -\alpha_1\left(\frac{1}{2R_i} - \frac{R_i}{A_i^2}\right) - \frac{\alpha_2}{2R_i}, \\ \xi_2^* = -\alpha_1\frac{X_i}{A_i^2}, \\ -R_i\xi_1^* + X_i\xi_2^* = \frac{1}{2A_0^2 A_i^2}\left(F_{lim}^2 - w_0^2 S_{lim}^2 A_i^2\right) \\ \left(\xi_1^* + \frac{1}{2R_i}\right)^2 + (\xi_2^*)^2 = \frac{w_0^2 S_{lim}^2}{A_0^2} \end{cases}$$

thus, by substituting the first two equations into the third one

$$\begin{cases} \xi_1^* = -\alpha_1\left(\frac{1}{2R_i} - \frac{R_i}{A_i^2}\right) - \frac{\alpha_2}{2R_i}, \\ \xi_2^* = -\alpha_1\frac{X_i}{A_i^2}, \\ \alpha_2 = \alpha_1 + \frac{1}{A_0^2 A_i^2}\left(F_{lim}^2 - w_0^2 S_{lim}^2 A_i^2\right) \\ \left(\xi_1^* + \frac{1}{2R_i}\right)^2 + (\xi_2^*)^2 = \frac{w_0^2 S_{lim}^2}{A_0^2} \end{cases}$$

By substituting the first three equations into the last one, one obtains a quadratic polynomial equation of α_1. This equation has two solutions. By considering the conditions $0 \leq \alpha_1 < 1$, $0 \leq \alpha_2 < 1$, it gets $\alpha_1 = \alpha$. It follows that $\xi_1^* = c_1, \xi_2^* = c_2$. Note that we have case 4 if and only conditions for other cases do not hold. The proof is complete. □

Appendix D. (Proof of Theorem 4): Problem (33), (34), (35) is feasible if and only if the feasible set is not-empty. This is equivalent to the condition

$$d^* \leq \frac{F_{lim}^2}{A_0^2 A_i^2} \tag{59}$$

where d^* is the minimum of the following optimization problem

$$\begin{aligned} &\min_{\xi} \left\{\left(\xi_1 + \frac{1}{2R_i} - \frac{R_i}{A_i^2}\right)^2 + \left(\xi_2 + \frac{X_i}{A_i^2}\right)^2\right\} \\ &\text{s.t. } \left(\xi_1 + \frac{1}{2R_i}\right)^2 + \xi_2^2 \leq \frac{w_0^2 S_{lim}^2}{A_0^2} \end{aligned} \tag{60}$$

The Lagrangian of (60) is given as

$$\begin{aligned} \mathcal{L}(\xi, \lambda) \quad &= \left(\xi_1 + \frac{1}{2R_i} - \frac{R_i}{A_i^2}\right)^2 + \left(\xi_2 + \frac{X_i}{A_i^2}\right)^2 \\ &+\lambda\left(\left(\xi_1 + \frac{1}{2R_i}\right)^2 + \xi_2^2 - \frac{w_0^2 S_{lim}^2}{A_0^2}\right) \end{aligned} \tag{61}$$

Using Karush-Kuhn-Tucker conditions, the optimal solution satisfies $\lambda^* \geq 0$, and

$$\begin{cases} \frac{\partial \mathcal{L}}{\partial \xi_1} = 2\left(\xi_1^* + \frac{1}{2R_i} - \frac{R_i}{A_i^2}\right) + 2\lambda^*\left(\xi_1^* + \frac{1}{2R_i}\right) = 0, \\ \frac{\partial \mathcal{L}}{\partial \xi_2} = 2\left(\xi_2^* + \frac{X_i}{A_i^2}\right) + 2\lambda^*\xi_2^* = 0, \\ \lambda^*\left(\left(\xi_1^* + \frac{1}{2R_i}\right)^2 + (\xi_2^*)^2 - \frac{w_0^2 S_{lim}^2}{A_0^2}\right) = 0 \end{cases}$$

or, equivalently

$$\begin{cases} \xi_1^* = -\frac{1}{2R_i} + \frac{1}{1+\lambda^*}\frac{R_i}{A_i^2}, \\ \xi_2^* = \frac{-1}{1+\lambda^*}\frac{X_i}{A_i^2}, \\ \lambda^*\left(\left(\xi_1^* + \frac{1}{2R_i}\right)^2 + (\xi_2^*)^2 - \frac{w_0^2 S_{lim}^2}{A_0^2}\right) = 0 \end{cases} \tag{62}$$

There are two cases.

Case 1: The constraint in (60) is inactive. In this case $\lambda^* = 0$, and

$$\begin{aligned} \xi_1^* &= -\frac{1}{2R_i} + \frac{R_i}{A_i^2}, \\ \xi_2^* &= -\frac{X_i}{A_i^2} \end{aligned}$$

Hence $d^* = 0$. Clearly, the inequality (59) is satisfied. We have case 1 if and only if

$$\left(\xi_1^* + \frac{1}{2R_i}\right)^2 + (\xi_2^*)^2 \leq \frac{w_0^2 S_{lim}^2}{A_0^2}$$

or, equivalently

$$\frac{R_i^2}{A_i^4} + \frac{X_i^2}{A_i^4} \leq \frac{w_0^2 S_{lim}^2}{A_0^2}$$

Recall that $R_i^2 + X_i^2 = A_i^2$. It follows that

$$A_0^2 \leq w_0^2 A_i^2 S_{lim}^2 \tag{63}$$

Hence if (40) holds then (63) is satisfied.

Case 2: The constraint in (60) is active. In this case $\lambda^* > 0$. Substituting the first two equations into the third one of (62), one obtains

$$\frac{1}{(1+\lambda^*)^2 A_i^2} = \frac{w_0^2 S_{lim}^2}{A_0^2}$$

Hence

$$\frac{1}{1+\lambda^*} = \frac{w_0 A_i S_{lim}}{A_0} \tag{64}$$

Using (62), (64), one obtains

$$\begin{aligned} \xi_1^* &= -\tfrac{1}{2R_i} + \tfrac{w_0 A_i S_{lim}}{A_0} \tfrac{R_i}{A_i^2}, \\ \xi_2^* &= -\tfrac{w_0 A_i S_{lim}}{A_0} \tfrac{X_i}{A_i^2} \end{aligned}$$

Therefore

$$\begin{aligned} d^* &= \left(\xi_1^* + \tfrac{1}{2R_i} - \tfrac{R_i}{A_i^2}\right)^2 + \left(\xi_2^* + \tfrac{X_i}{A_i^2}\right)^2 \\ &= \left(1 - \tfrac{w_0 A_i S_{lim}}{A_0}\right)^2 \left(\tfrac{R_i^2}{A_i^4} + \tfrac{X_i^2}{A_i^4}\right) \\ &= \tfrac{(A_0 - w_0 A_i S_{lim})^2}{A_0^2 A_i^2} \end{aligned}$$

Using (59), one has $|A_0 - w_0 A_i S_{lim}| \leq F_{lim}$. Note that we have case 2 if and only if condition (63) is not satisfied. Hence $A_0 \geq w_0 A_i S_{lim}$. It follows that $A_0 - w_0 A_i S_{lim} \leq F_{lim}$. This is the condition (40). The proof is complete. □

Hoai-Nam Nguyen received the engineering degree from Bauman, Moscow State Technical University, Russia in 2009, and the Ph.D. degree from École Supérieure d'Électricité, Supelec, Gif-sur-Yvette, France in 2012. After two years of postdoc, he spent 7 years in industry at IFP Energies Nouvelles as a research engineer. Since September, 2021, he works at Télécom SudParis, Institut Polytechnique de Paris as an associate professor. His main research interests are optimization based control, sensor fusion, embedded systems, renewable energies.